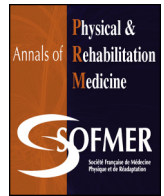




Available online at
ScienceDirect
www.sciencedirect.com

Elsevier Masson France
EM|consulte
www.em-consulte.com



Original article

Synergic regenerative effects of polydeoxyribonucleotide and microcurrent on full-thickness rotator cuff healing in a rabbit model

Q1 Dong Rak Kwon^{a,*}, Yong Suk Moon^b

^a Department of Rehabilitation, School of Medicine, Catholic University of Daegu School of Medicine, 33 Duryugongwon-ro 17-gil, Nam-Gu, Daegu, South Korea

^b Department of Anatomy, School of Medicine, Catholic University of Daegu School of Medicine, 33 Duryugongwon-ro 17-gil, Nam-Gu, Daegu, South Korea

ARTICLE INFO

Article history:

Received 18 February 2019

Accepted 2 September 2019

Keywords:

Shoulder
Rotator cuff
Microcurrent
Polydeoxyribonucleotide
Injections
Ultrasonography

ABSTRACT

Background: Rotator cuff tendon tears (RCTTs) are common adult injuries. We hypothesized that a local injection of polydeoxyribonucleotide (PDRN) and microcurrent therapy (MIC) would be more effective in regenerating a tendon tear than PDRN administration alone.

Objectives: To evaluate the effect of PDRN combined with MIC on the regeneration of RCTTs in a rabbit subscapularis tendon chronic RCTT model.

Methods: Rabbits ($n = 24$) were allocated to 3 groups at 6 weeks after full-thickness RCTT (FTRCTT): 0.2 mL normal saline (G1-SAL); 0.2 mL PDRN with Sham MIC (G2-PDRN + Sham MIC); and 0.2 mL PDRN with MIC (G3-PDRN + MIC). All treatments were performed under ultrasound guidance. PDRN was injected weekly for 4 weeks and sham MIC or MIC was applied daily for 4 weeks after the first PDRN injection.

Results: In the G3-PDRN + MIC group, the mean (SD) subscapularis tendon tear size was continuously reduced from 1 week post-treatment to 4 weeks and was significantly decreased as compared with the other 2 groups [6.0 (1.5) vs. G1: 11.5 (1.8) and G2: 9.1 (1.6) mm²; G3 vs. G1, $P < 0.001$; G3 vs. G2, $P = 0.018$]. The gross morphologic mean tendon tear size was significantly smaller in the G3-PDRN + MIC group than G1-SAL and G2-PDRN + Sham MIC groups [8.8 (3.5) vs. 15.9 (2.3) and 12.4 (1.6) mm²; G3 vs. G1, $P < 0.001$; G3 vs. G2, $P = 0.03$]. Mean values for regenerated collagen type 1 fibers, angiogenesis, and walking parameters were all greater for the G3-PDRN + MIC group than the other 2 groups based on histological examination and motion analysis [collagen type 1, G3: 1.60 (0.80) vs. G1: 0.45 (0.60), G2: 1.10 (0.74), G3 vs. G1, $P < 0.001$; G3 vs. G2, $P = 0.002$] [angiogenesis, G3: 2.44 (0.73) vs. G1: 0.80 (0.82) and G2: 2.06 (0.81), G3 vs. G1, $P < 0.001$; G3 vs. G2, $P = 0.006$] [walking distance, G3: 6391.4 (196.9) vs. G1: 4852.8 (137.3) and G2: 5514.4 (257.3) cm; G3 vs. G1, $P < 0.001$; G3 vs. G2, $P < 0.001$].

Conclusions: On gross morphologic, histological, and motion analysis, combined PDRN with MIC therapy was more effective than PDRN alone treating a rabbit model of chronic traumatic FTRCTT.

© 2019 Elsevier Masson SAS. All rights reserved.

1. Introduction

Rotator cuff tendon tears (RCTTs) are the most common tendon injury in the adult population, affecting approximately 30% of the population older than 60 years [1]. Although the surgical repair of an RCTT is also one of the most common orthopedic procedures, the failure rate ranges widely, from 20% to 90% [2]. The unresolved

disadvantage of the current treatment approach has motivated efforts to repair RCTTs by using biological adjuvants.

For example, polydeoxyribonucleotide (PDRN), a mixture of deoxyribonucleotide polymers with chain lengths from 50 to 2000 bp, was recently reported to be effective in treating chronic rotator cuff disease [3]. PDRN induces angiogenesis and collagen synthesis and also possesses anti-inflammatory activity [4]. A recent animal study [5] showed that co-injection of umbilical cord blood-derived mesenchymal stem cells (UCB-MSCs) and PDRN was more effective for regeneration in a full-thickness RCTT (FTRCTT) than UCB-MSC injection alone. These effects are considered mediated by promoting vascular endothelial growth factor (VEGF) expression, which might have regeneration potential in RCTT.

* Corresponding author. Department of Rehabilitation Medicine, Catholic University of Daegu School of Medicine, 33 Duryugongwon-ro 17-gil, Nam-Gu, Daegu 42472, South Korea.

E-mail addresses: coolkwon@cu.ac.kr, dongrakkwon@hotmail.com (D.R. Kwon).

VEGF is a major growth factor that accelerates the healing process by stimulating new vessel formation in regions of poor circulation, including FTRCTT. VEGF regulates multiple biological functions of endothelial cells, thus enhancing the production of vasodilatory mediators, increasing vascular permeability, and stimulating their migration, proliferation, and formation [6].

In animal studies and clinical practice, the use of microcurrent stimulation could promote the release of VEGF in vitro [7,8]. Microcurrent therapy (MIC) involves the therapeutic application of a very low electric current (< 1 mA), which is usually sub-sensory to the body. MIC can also help provide the high energy supply required for the complex process of wound healing [9] by stimulating the production of adenosine triphosphate, which is required as an energy source for a very large number of intracellular biochemical processes and can thus accelerate wound healing.

Thus, we hypothesized that local injection of PDRN and MIC would be more effective in regeneration after a tendon tear than PDRN administration alone in an animal model. We evaluated the effect of PDRN combined with MIC on regeneration after an RCTT in a rabbit model of subscapularis tendon chronic RCTT.

2. Materials and methods

2.1. Animal model

Twelve-week-old male New Zealand white rabbits ($n = 24$) were housed in separate metal cages at $24 \pm 12^\circ\text{C}$ with relative humidity $45 \pm 10\%$. The animals had free access to tap water and were fed a commercial rabbit diet. None of the rabbits received additional exercise but were free to conduct normal activities in a $65 \times 45 \times 30$ -cm cage. The animal experiments were performed in accordance with internationally accredited guidelines and were approved by the Institutional Animal Care and Use Committee (IACUC) of the University School of Medicine. Anesthesia was induced with isoflurane (JW Pharmaceutical, Goyang, South Korea) vaporized in oxygen, delivered by using a large animal cycling system. With rabbits under general anesthesia, 5×5 -mm FTRCTTs were created just proximal to the insertion site on the left subscapularis tendon by using a 5-mm biopsy punch as described [10]. The procedure was

performed by a physiatrist with 20 years of animal study experience. Each excision wound was immediately covered with an unresorbable round silicone Penrose drainage tube (Sewoon Medical Co., Cheonan, South Korea) to induce a chronic rotator cuff tear [11]. The incision was closed by using subcutaneous and skin sutures.

2.2. Animal grouping and injection

Six weeks after the excisions, the inserted tubes were removed, and the site of each full-thickness subscapularis tendon tear was confirmed. The skin over the induced tendon rupture area was then resealed for injecting PDRN. Twenty-four rabbits were randomly allocated to 3 treatment groups by computerized random numbers ($n = 8$ per group): 0.2 mL normal saline (G1-SAL group); 0.2 mL PDRN with sham MIC (G2-PDRN + Sham MIC group); and 0.2 mL PDRN with MIC (G3-PDRN + MIC group). Normal saline or PDRN was injected into the site of the FTRCTT under ultrasonography (US) guidance. MIC was applied to the surface of the site of the FTRCTT. Rabbits were injected with commercially obtained PDRN (Placentex integro, Mastelli S.r.l., San Remo, Italy) once a week for 4 weeks, and sham MIC or MIC was applied daily for 1 hr for 4 weeks after the first PDRN injection. The concentration of PDRN was 1.875 mg/mL. MIC was applied by attaching the electrical pad to the skin surface of the injury site and using the MIC generator device (intensity 25 μA , frequency 8 Hz; Granthe; Cosmic Co., Seoul, Korea). Sham MIC was applied by attaching the electrical pad to the skin surface of tear site. The appearance of the sham MIC was identical to the real stimulator but without an electrical current, even when it was operational.

All 24 rabbits were euthanized at 4 weeks after the first injection (Fig. 1). The subscapularis tendon tear size (STTS) was measured by US at baseline (pre-treatment) and at 1, 2, 3, and 4 weeks post-treatment. All injections and US measurements were performed under US guidance by a physiatrist with 15 years of musculoskeletal US experience who used an EPIQ 5 system with an 18- to 5-MHz multi-frequency linear transducer (Philips Healthcare, Andover, MA, USA). The physiatrist was blinded to allocated group. No medication was administered during the procedure. All rabbits were immobilized in the equinus position by use of an elastic bandage for 2 days after the injection.

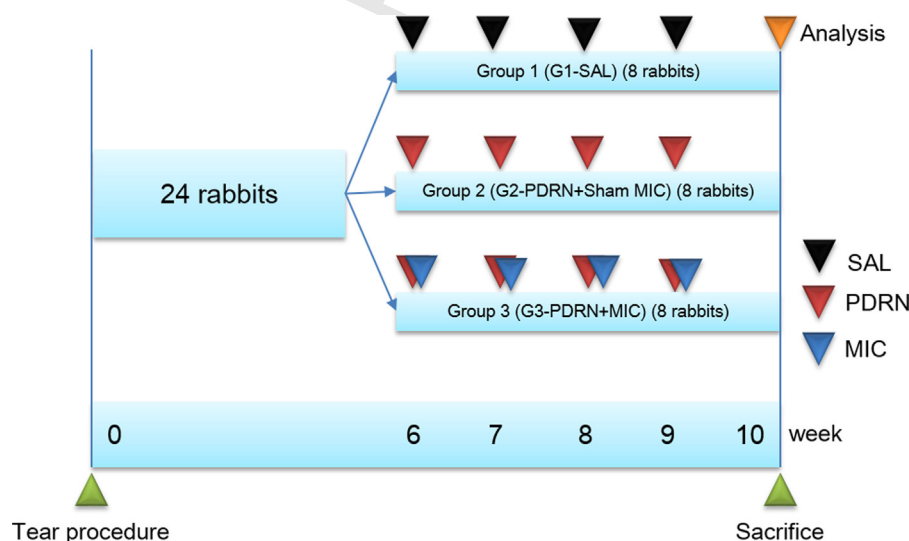


Fig. 1. Timeline of saline (SAL), polydeoxyribonucleotide acid (PDRN) with Sham microcurrent therapy (MIC), and PDRN with MIC. G1-S, 0.2 mL normal saline; G2-PDRN + Sham MIC was injected with 0.2 mL PDRN, once a week for 4 weeks under ultrasonography guidance into the left shoulder subscapularis full-thickness tears at 6 weeks after tears were created and sham MIC for 4 weeks after the first PDRN injection. G3-PDRN + MIC was injected with 0.2 mL PDRN, once a week for 4 weeks and MIC was applied daily for 1 h for 4 weeks. All rabbits were euthanized by carbon monoxide inhalation 4 weeks after the first solution injection, and gross morphology of the tear site, histologic examination, and motion analysis were performed. SAL, 0.2 mL normal saline; PDRN, polydeoxyribonucleotide acid; MIC, microcurrent therapy.

2.3. Gross morphology examination

Gross morphologic examinations were conducted after each rabbit was euthanized. One assessor measured the tear site with blinding to allocated group. Each tendon tear was classified as partial or full thickness. A full-thickness tear was defined as a tear involving the whole full-thickness tendon; otherwise, it was a partial-thickness tear. The subscapularis tendon tear was photographed along with a clear plastic ruler placed near the center of the tear site to permit size measurements by using ImageJ software (US National Institutes of Health, Bethesda, MD, USA) by tracing the outlined tear edge pre-treatment and at 4 weeks post-treatment.

2.4. Histological examination

2.4.1. Tissue preparation

Rabbits were sacrificed under general anesthesia after all intramuscular injections. The tear area of the subscapularis tendon was segmented and fixed with neutral buffered formalin for 24 hr. Each specimen was embedded in paraffin (Paraplast; Oxford, St. Louis, MO, USA), and sagittal slices were created to obtain 5- μ m-thick serial sections, which were stained with Masson's trichrome (MT) and examined by light microscopy.

2.4.2. Immunohistochemistry

Tendon sections were immunohistochemically stained with the mouse monoclonal antibody anti-collagen 1 (COL-1; Abcam, Cambridge, UK), a marker of collagen fibers; mouse monoclonal antibody anti-proliferating cell nuclear antigen (PCNA, PC10; Santa Cruz Biotechnology, Santa Cruz, CA, USA), a marker of proliferating cells; and the angiogenic markers anti-VEGF (A-20) and anti-platelet endothelial cell adhesion molecule-1 polyclonal antibody (PECAM-1, M-20, both Santa Cruz Biotechnology). Paraffin-embedded sections were then cleared, dehydrated, and washed with phosphate buffered saline (PBS). Antigen retrieval involved using ethylenediaminetetraacetic acid (EDTA) buffer (1 mM EDTA, pH 8.0) for 30 min at 95 °C, followed by cooling. Endogenous peroxidases were inhibited by pre-incubation with 0.3% hydrogen peroxide (H₂O₂) in PBS for 30 min. Non-specific protein binding was blocked in PBS containing 10% normal horse serum, goat serum, or rabbit serum (Vector Laboratories, Burlingame, CA, USA) for 30 min. These sections were then incubated with the primary antibodies (1:100–1:200) at room temperature for 2 hr and washed 3 times with PBS. The secondary antibody (1:100), biotinylated anti-mouse, anti-rabbit, or anti-goat IgG (Vector Laboratories), was placed on sections and incubated at room temperature for 1 hr. After washing with PBS 3 times, sections were exposed to avidin-biotin-peroxidase complex (Vector Laboratories) for 1 hr, washed 3 times with PBS, and subjected to a peroxidase reaction with 0.05 M Tris-HCl (pH 7.6) containing 0.01% H₂O₂ and 0.05% 3,3'-diaminobenzidine (Sigma-Aldrich). These sections were counterstained with hematoxylin, then mounted. Negative controls were sections with no primary antibody staining. Skin sections were positive controls. The slides were examined under an Axiophot Photomicroscope (Carl Zeiss, Germany) equipped with an AxioCam MRc5 camera (Carl Zeiss, Germany).

2.4.3. Evaluation of immunohistochemical staining

Each slide was evaluated according to the intensity of positive immunostaining. The single reader was blinded to the allocated group. In total, 30 randomly selected fields from each group were photographed as described above, and AxioVision SE64 (Carl Zeiss, Germany) was used for analysis. A widely adopted semi-quantitative scoring system was used for the nuclear or

cytoplasmic markers PCNA, VEGF, and PECAM-1, considering both the staining intensity and extent of area as reported previously [12,13]. In brief, the proportion of positively stained cells was scored as 0 (no cells stained positive), 1 (1–10% positive cells), 2 (11–33% positive cells), 3 (34–66% positive cells), or 4 (67–100% positive cells). The intensity of COL-1 or MT staining was classified as 0, negative staining; 1, slight positive staining; 2, moderately positive staining; or 3, strongly positive staining.

2.5. Motion analysis

Motion analysis of the rabbits was conducted at pre-injection and 4 weeks post-injection. One assessor performed the motion analysis and was blinded to the allocated group. The rabbits were habituated to the open test field in a 3 \times 3-m arena for 30 min before motion analysis. They were then allowed to freely explore the field for 5 min. Their movements were individually assessed by using a video-tracking system equipped with a camera (Smart; Panlab, Barcelona, Spain) that recorded the rabbit's horizontal activity. The 5-min walking distance, fast walking time, and mean walking speed were measured.

2.6. Statistical analyses

All statistical analyses were performed with SPSS for Windows, v19.0 (SPSS Inc., Chicago, IL, USA). In addition to standard descriptive statistical calculations (means and standard deviations), ANOVA and the Kruskal-Wallis test were used to determine statistical differences within and among groups. When ANOVA and the Kruskal-Wallis test yielded significant results, Tukey's test and the Mann-Whitney test were also performed to assess pair-wise differences between groups. Data are reported as mean values and 95% confidence intervals. Bonferroni correction was used to control for multiple comparisons. Statistically significant level was determined at $P < 0.05$.

3. Results

3.1. Gross morphology

In the G3-PDRN + MIC group, the mean STTS was continuously reduced from 1 week post-treatment up to 4 weeks and was significantly decreased as compared with the other two groups [G3: 6.0 (1.5) vs. G1: 11.5 (1.8) and G2: 9.1 (1.6) mm²; G3 vs. G1, $P < 0.001$; G3 vs. G2, $P = 0.018$] (Table 1). At 4 weeks post-treatment, the mean STTS was significantly smaller in the G2-PDRN + Sham MIC than G1-SAL group ($P < 0.001$, Fig. 2). In

Table 1

Subscapularis tendon tear size (mm²) measured in rabbits by using ultrasound. Measurements were performed at baseline (pre-treatment) and at 1, 2, 3, and 4 weeks post-treatment.

	G1-SAL (n = 8)	G2-PDRN + Sham MIC (n = 8)	G3-PDRN + MIC (n = 8)
Pre-treatment	12.3 (2.4)	13.1 (1.4)	12.1 (1.5)
1 week	11.9 (2.0)	12.1 (1.1)*	9.7 (1.2)* ^{a,b}
2 week	11.6 (1.8)	11.1 (1.1)*	8.1 (1.0)* ^{a,b}
3 week	11.5 (1.8)	10.1 (1.3)*	7.3 (1.2)* ^{a,b}
4 week	11.5 (1.8)	9.1 (1.6)* ^{a,c}	6.0 (1.5)* ^{a,b}

Data are mean (SD). G1-SAL: 0.2 mL normal saline; G2-PDRN + Sham MIC: 0.2 mL PDRN with sham MIC; G3-PDRN + MIC: 0.2 mL PDRN with MIC. SAL: Normal saline; PDRN: polydeoxyribonucleotide; MIC: microcurrent therapy.

* $P < 0.05$, derived from repeated measures ANOVA for effect of time.

^a $P < 0.05$ between groups 1 and 3 by one-way ANOVA, Tukey's post hoc test.

^b $P < 0.05$ between groups 2 and 3 by one-way ANOVA, Tukey's post hoc test.

^c $P < 0.05$ between groups 1 and 2 by one-way ANOVA, Tukey's post hoc test.

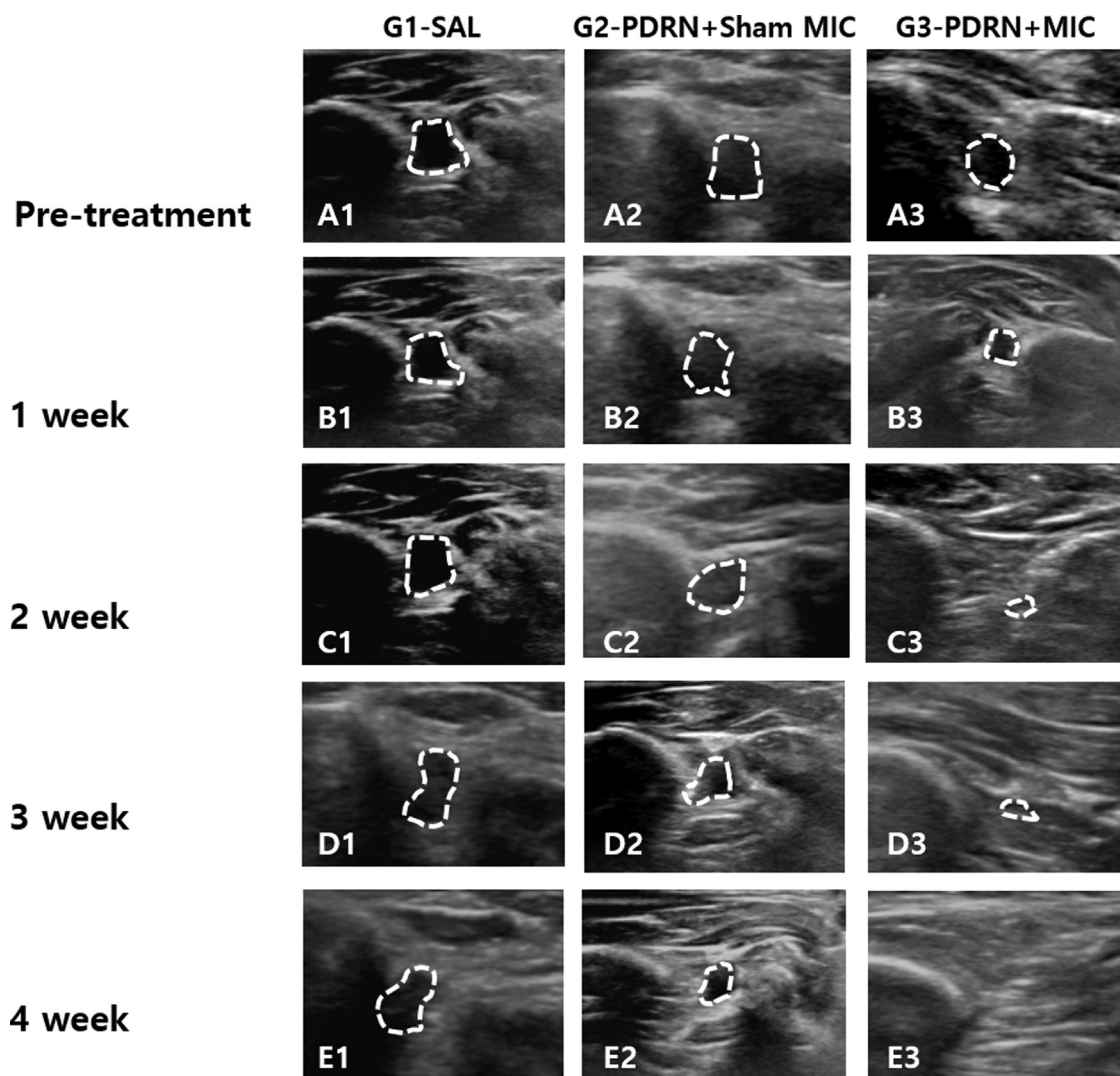


Fig. 2. Sequential changes in ultrasonography findings of subscapularis tendon tear at pre-treatment and 1, 2, 3 and 4 weeks post-treatment. Ultrasonography (A1–E3) findings of the subscapularis tendons in G1-SAL, G2-PDRN + Sham MIC, and G3-PDRN + MIC groups.

the G1-SAL group, a full-thickness tendon tear was observed in all 8 (100%) rabbits at 4 weeks post-treatment. However, in the G2-PDRN + Sham MIC and G3-PDRN + MIC groups, a full-thickness tendon tear was observed in only 5 (62.5%) and 3 (37.5%) rabbits, respectively, and a partial-thickness subscapularis tendon tear was observed in 3 (37.5%) and 4 (50%) rabbits. Moreover, one of the rabbits (12.5%) in the G3-PDRN + MIC group showed nearly complete healing (Fig. 3). The mean tendon tear size was significantly smaller in the G3-PDRN + MIC than G1-SAL and G2-PDRN + Sham MIC groups [G3: 8.8 (3.5) vs. G1: 15.9 (2.3) and G2: 12.4 (1.6) mm²; G3 vs. G1, $P < 0.001$; G3 vs. G2, $P = 0.03$; Table 2, Fig. 4, Fig. 5].

3.2. Histology and immunohistochemistry

MT staining clearly showed regenerated collagen fibers, which stained positively for COL-1 in the G1-SAL, G2-PDRN + Sham MIC, and G3-PDRN + MIC groups (Fig. 6, A1–A3). However, the MT-stained fiber and COL-1-positive cell densities were significantly greater for the G3-PDRN + MIC than the other 2 groups (MT, G3: 1.53 (0.93) vs. G1: 0.38 (0.49) and G2: 0.98 (0.86); G3 vs. G1, $P < 0.001$; G3 vs. G2, $P = 0.013$) (COL-1, G3: 1.60 (0.80) vs. G1: 0.45 (0.60) and G2: 1.10 (0.74); G3 vs. G1, $P < 0.001$; G3 vs. G2,

$P = 0.002$, Fig. 6, B1–B3; Table 2). Extensive PCNA staining was also observed in the regenerated collagen fibers in the G2-PDRN + Sham MIC and G3-PDRN + MIC groups (Fig. 6, C1–C3).

Immunohistochemistry staining revealed numerous VEGF-positive cells. PECAM-1-positive microvascular density was significantly higher in the G2-PDRN + Sham MIC and G3-PDRN + MIC groups than G1-SAL group (Fig. 6, D1–E3). The intensity of PCNA staining and the number of VEGF-positive and PECAM-1 positive cells were significantly higher in the G3-PDRN + MIC than the other 2 groups (PCNA, G3: 2.94 (0.81) vs. G1: 1.04 (0.91) and G2: 2.53 (0.95); G3 vs. G1, $P < 0.001$; G3 vs. G2, $P = 0.013$) (VEGF, G3: 2.44 (0.73) vs. G1: 0.80 (0.82) and G2: 2.06 (0.81); G3 vs. G1, $P < 0.001$; G3 vs. G2, $P = 0.006$) (PECAM-1, G3: 2.58 (0.71) vs. G1: 1.45 (1.06) and G2: 2.24 (0.70); G3 vs. G1, $P < 0.001$; G3 vs. G2, $P = 0.005$, Table 2, Fig. 7).

3.3. Motion analyses

In the motion analysis, walking distance, fast walking time, and mean walking speed were significantly greater in the G2-PDRN + Sham MIC and G3-PDRN + MIC groups than the G1-SAL group (walking distance, G2: 5514.4 (257.3) and G3: 6391.4 (196.9) vs. G1: 4852.8 (137.3) cm; G2 vs. G1, $P < 0.001$; G3 vs. G1,

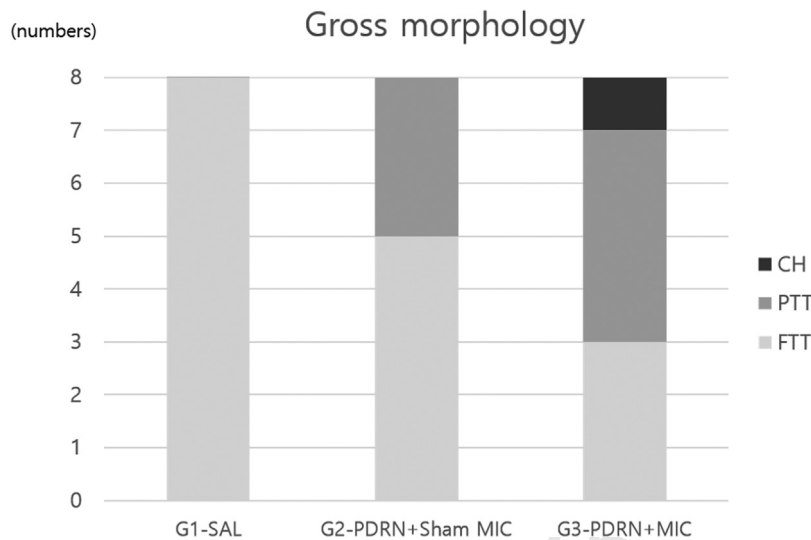


Fig. 3. Gross morphology of tear site at 4 weeks post-treatment. In the G1-SAL group, a full-thickness tendon tear (FTT) was observed in every rabbit. In the G2-PDRN + Sham MIC group, a partial-thickness tendon tear (PTT) was observed in 3 rabbits and an FTT in 5 rabbits. In the G3-PDRN + MIC group, a PTT was observed in 4 rabbits, an FTT in 3 rabbits, and complete healing (CH) in 1 rabbit.

Table 2

Semiquantitative score of gross morphologic, histological findings, immunoreactivity of staining and motion analysis by treatment group at 4 weeks post-treatment.

	G1-SAL (n = 8)	G2-PDRN + Sham MIC (n = 8)	G3-PDRN + MIC (n = 8)
Gross			
Tear size (mm ²)	15.9 (2.3)	12.4 (1.6)*	8.8 (3.5) ^{a,b}
Histological score			
MTS	0.38 (0.49)	0.98 (0.86) ^c	1.53 (0.93) ^{d,e}
COL-1	0.45 (0.60)	1.10 (0.74) ^c	1.60 (0.80) ^{d,e}
PCNA	1.04 (0.91)	2.53 (0.95)*	2.94 (0.81) ^{a,b}
VEGF	0.80 (0.82)	2.06 (0.81)*	2.44 (0.73) ^{a,b}
PECAM-1	1.45 (1.06)	2.24 (0.70)*	2.58 (0.71) ^{a,b}
Motion analysis			
Walking distance (cm)	4852.8 (137.3)	5514.4 (257.3)*	6391.4 (196.9) ^{a,b}
Fast walking time (%)	5.6 (1.4)	8.0 (0.8)*	10.9 (1.1) ^{a,b}
Mean walking speed (cm/sec)	6.3 (0.6)	8.2 (0.6)*	12.0 (1.5) ^{a,b}

Data are mean (SD). G1-SAL: 0.2 mL normal saline; G2-PDRN + Sham MIC: 0.2 mL PDRN with sham MIC; G3-PDRN + MIC: 0.2 mL PDRN with MIC. The intensity of MIC staining or COL-1 immunostaining was classified as 0, negative staining; 1, slight positive staining; 2, moderately positive staining; or 3, strongly positive staining. The proportion of cells positive for PCNA, VEGF, PECAM-1 was scored as 0, no cells stained positive; 1, 1% to 10% stained; 2, 11% to 33% stained; 3, 34% to 66% stained; 4, 67% to 100% stained. PDRN: polydeoxyribonucleotide; MIC: microcurrent therapy; MTS: Masson's trichrome stain; COL-1: anti-type 1 collagen antibody; PCNA: proliferating cell nuclear antigen; VEGF: vascular endothelial growth factor; PECAM-1: platelet endothelial cell adhesion molecule.

* $P < 0.05$ between group 1 and 2 by one-way ANOVA, Tukey's post hoc test.

^a $P < 0.05$ between group 1 and 3 by one-way ANOVA, Tukey's post hoc test.

^b $P < 0.05$ between group 2 and 3 by one-way ANOVA, Tukey's post hoc test.

^c $P < 0.016$ between group 1 and 2 by Kruskal-Wallis, Mann-Whitney test.

^d $P < 0.016$ between group 1 and 3 by Kruskal-Wallis, Mann-Whitney test.

^e $P < 0.016$ between group 2 and 3 by Kruskal-Wallis, Mann-Whitney test.

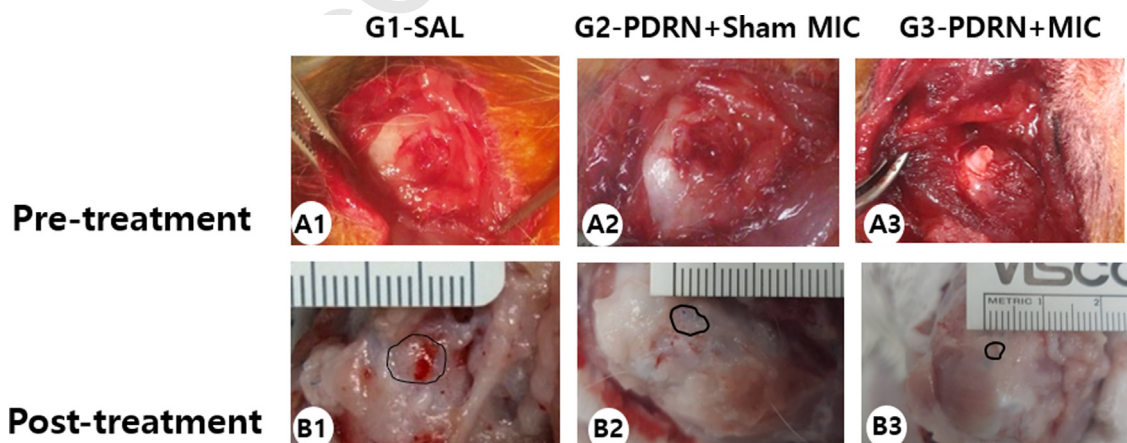


Fig. 4. Gross morphology. Gross morphological (A1–B3) findings of the subscapularis tendons in G1-SAL, G2-PDRN + Sham MIC, and G3-PDRN + MIC groups.

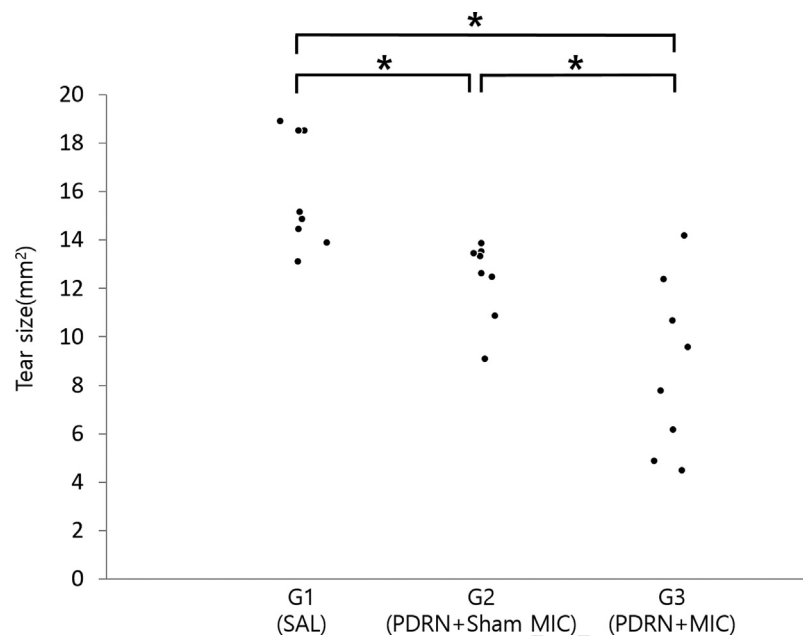


Fig. 5. Subscapularis tendon tear size on gross morphology at 4 weeks post-treatment. * $P < 0.05$, one-way ANOVA, Tukey's post-hoc test between two groups.

$P < 0.001$) (fast walking time, G2: 8.0% (0.8) and G3: 10.9% (1.1) vs. G1: 5.6% (1.4); G2 vs. G1, $P = 0.002$; G3 vs. G1, $P < 0.001$) (mean walking speed, G2: 8.2 (0.6) and G3: 12.0 (1.5) vs. G1: 6.3 (0.6) cm/sec; G2 vs. G1, $P = 0.002$; G3 vs. G1, $P < 0.001$, Table 2, Fig. 8). In addition, walking distance, fast walking time, and mean walking speed were greater in the G3-PDRN + MIC group than the other 2 groups (walking distance: G3 vs. G2; mean walking time: G3 vs. G2; mean walking speed: G3 vs. G2, all $P < 0.001$, Table 2, Fig. 8).

4. Discussion

Given the additional energy input, we hypothesized that local injection of PDRN with MIC would be more effective for repair of a tendon tear than PDRN administration alone in an animal model. Indeed, rabbits with PDRN and MIC combined showed reduced tendon tear size, with enhanced newly regenerated collagen type 1 fibers, cell proliferation, angiogenesis, walking distance, and fast walking time, than those with PDRN alone.

Low cell density in the tendon tissue and minimal blood supply leads to limited extracellular matrix restoration for tendon healing. Conservative approaches avoiding anatomical reduction are generally used to achieve tendon healing based on external mechanical stimulation [14,15], which could enhance cells synthesizing extracellular matrix components and cytokines to promote cell proliferation.

Similar to other electrotherapies, the therapeutic effect of MIC is also intensity-dependent. Previous studies have demonstrated that low-intensity electrotherapy improves the healing of damaged tendons and ligaments [16–20]. When an intensity of 100–500 μA was applied for treating muscle damage, the healing processes, including amino acid transport, triphosphate generation, and protein synthesis, were increased by 30% to 40% above the control level; however, these bio-stimulatory effects were reversed when the intensity exceeded 1000 μA [16]. Dunn [20] demonstrated the growth of fibroblasts in the collagen matrix in an experimental skin wound in guinea pig by using electric currents from 20 to 100 μA , with the maximum fibroblast-growth response observed near the cathode, although different MIC machines were used. A recent study compared the effectiveness of MIC with two

different electric current intensities (50 vs. 500 μA) and suggested that a peak current intensity of 50 μA was more effective than 500 μA in reducing symptoms and promoting tendon normalization in chronic tennis elbow [12]. These current intensities are within the range found optimal for adenosine triphosphate generation. The results of our study agree with these previous findings, suggesting that low-amperage currents promote tissue regeneration.

Moreover, other studies [21,22] demonstrated that low frequencies were more efficient in promoting the repair of connective tissues because they act by altering the membrane potentials of the cell. We found that electrical stimulation with MIC (intensity 25 μA , frequency 8 Hz) for 60 min/day for 4 weeks could reduce the size of a rotator cuff tear (G1-SAL group: 45%; G2-PDRN + Sham MIC: 30%) in an FTRCTT rabbit model. We chose to apply the MIC for 4 weeks because our previous clinical experience showed that this duration was well tolerated by patients. In addition, another study demonstrated that a peak current intensity of 50 μA for more than 3 weeks was needed to reduce symptoms and promote tendon normalization in chronic tennis elbow [12]. Although longer treatment times have been associated with greater success in trials of MIC with other tissue types [12], we did not assess the effects of treatment time on the outcome. As expected, we observed no adverse effects or untoward events because MIC works at the microampere level and mimics the electrical intensity found in living tissues [21,23].

Low immunogenicity and safety are also attractive characteristics of PDRN. PDRN is available as a pharmaceutical product for injection. Because the regenerative effect of PDRN is not dose-dependent and increasing the volume of PDRN would not likely result in better therapeutic effects, its combination with MIC is more compelling.

Current regeneration strategies for RCTT mainly consist of therapies based on bioactive scaffolds with the use of cells and signaling molecules [24]. During tissue regeneration, cell growth and differentiation, neovascularization, collagen synthesis, inflammatory response, and proteinase activity should be controlled [25]. PDRN, along with the nucleotides and nucleosides resulting from its degradation, can stimulate cell migration and growth, extracellular matrix protein production, and reduce inflammation

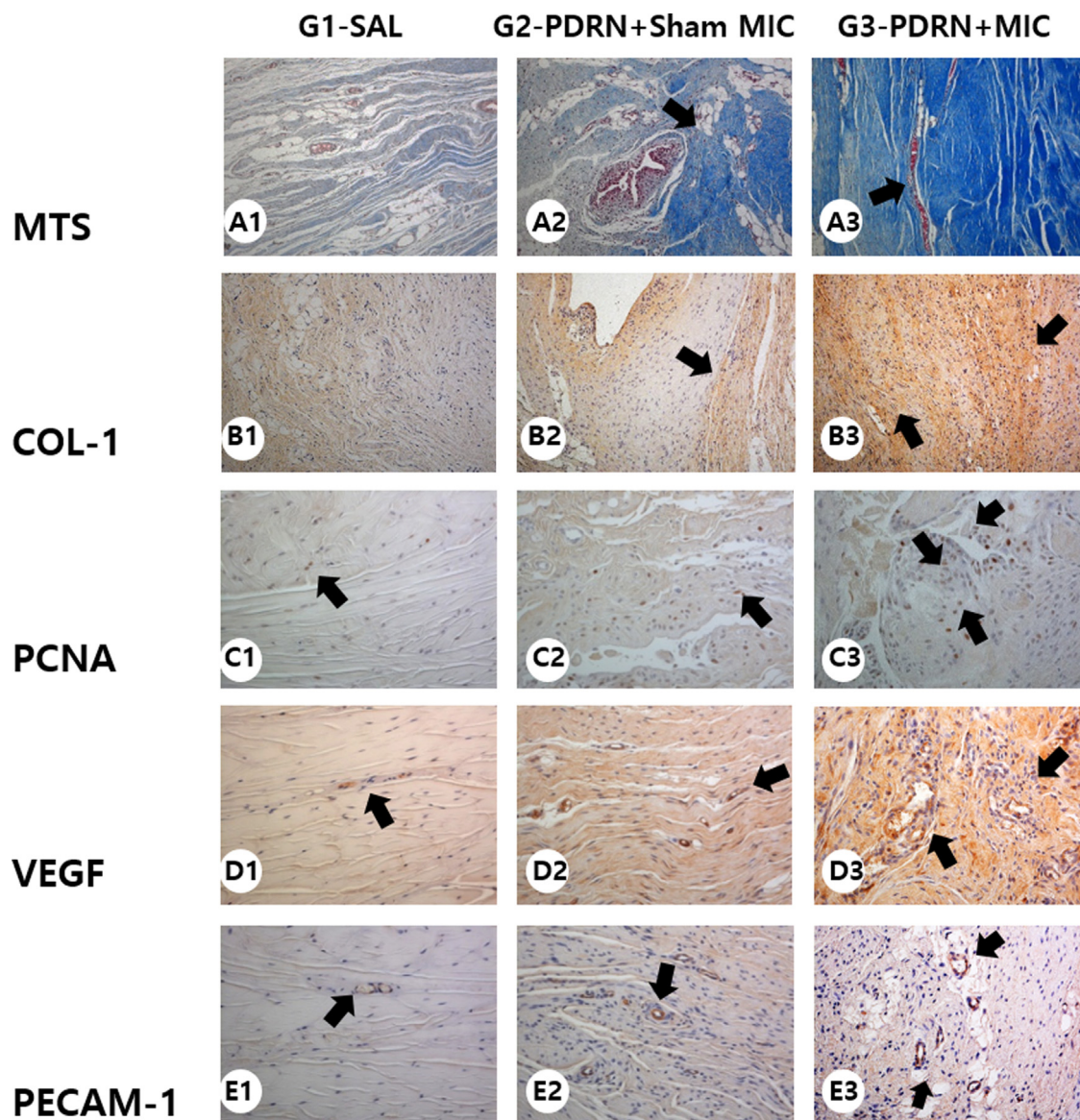


Fig. 6. Immunohistochemical findings. Immunohistochemical (A1–E3) findings of the subscapularis tendons in G1-SAL, G2-PDRN + Sham MIC, and G3-PDRN + MIC groups. (A1–A3) Newly regenerated tendons are shown in the blue-stained fibers (black arrow; Masson's trichrome stain; $\times 200$) in G2-PDRN + Sham MIC and G3-PDRN + MIC groups. Few regenerative collagen fibers were seen in the G1-SAL group. (B1–B3) Regenerated tendon fibers (black arrow; $\times 200$) were stained with anti-type 1 collagen antibody in G2-PDRN + Sham MIC and G3-PDRN + MIC groups. Few regenerated tendon fibers were seen in the G1-SAL group. (C1–C3) Numerous PCNA stained cells (black arrow, $\times 200$) were observed in regenerated tendon fibers in G2-PDRN + Sham MIC and G3-PDRN + MIC groups. Few PCNA stained cells were observed in the G1-SAL group (D1–E3) Numerous VEGF-positive cells and PECAM-1-positive microvascular densities (black arrows, $\times 200$) were observed in G2-PDRN + Sham MIC and G3-PDRN + MIC groups. Few VEGF-positive cells and PECAM-1 positive microvascular densities were observed in the G1-SAL group. MTS: Masson's trichrome stain; COL-1: Anti-type 1 collagen stain; PCNA: proliferating cell nuclear antigen; VEGF: vascular endothelial growth factor; and PECAM: platelet endothelial cell adhesion molecule.

[22]. Moreover, PDRN can penetrate the cell via different transport mechanisms to provide purine and pyrimidine rings that can be used by enzymes of salvage pathways, thus stimulating the synthesis of nucleic acids with a significant energy-saving mechanism [26]. Purine nucleotides and nucleosides can bind to specific receptors and trigger different signal transduction pathways, acting as mitogens for fibroblasts, endothelial cells, and neuroglia [27,28] and exhibiting synergistic effects with different growth factors [29,30]. Because of their safety, low production costs, absence of systemic toxicity, and antigenicity signs, PDRNs are currently widely used in clinical practice for bone, cartilage, and tendon diseases [31].

However, the optimal dose of PDRN required for regenerating the rotator cuff has not yet been established. A half-vial of PDRN (1.5 mL) has been injected weekly for 3 weeks for treating plantar

fasciitis [4], whereas 5.625 mg in 3 mL of PDRN has been injected at weekly intervals for 3 weeks to treat chronic rotator cuff tendinopathy [3]. We used four 0.2-mL weekly injections (total of 0.8 mL) of PDRN in the present study because the weight of a rabbit is approximately 5% that of a typical human adult.

PDRN increases VEGF expression by stimulating the adenosine A_{2A} receptor. VEGF is an angiogenic factor that can induce angiogenesis and collagen synthesis [32,33] and is thus a major growth factor that accelerates the healing process by stimulating new vessel formation in poor circulatory areas such as a diabetic foot. Therefore, it could also help increase the healing process in degenerative tissue that involves poor circulation. Indeed, immunohistochemistry staining revealed numerous VEGF-positive cells, and the PECAM-1-positive microvascular densities were significantly larger in the G3-PDRN + MIC than G2-PDRN + Sham

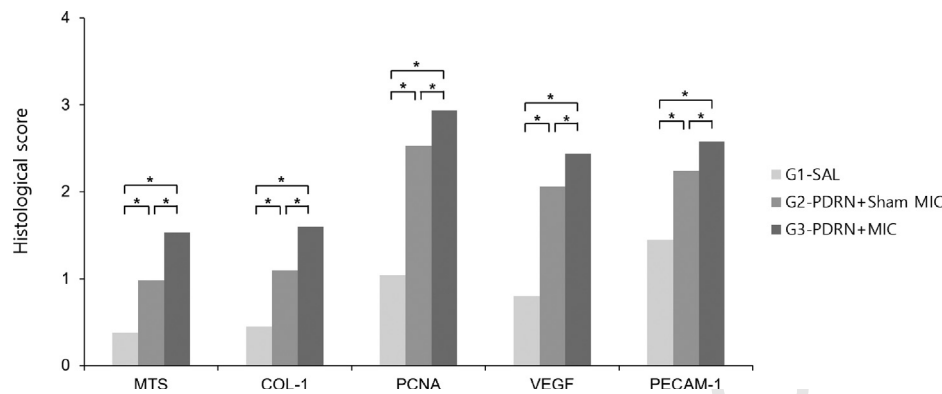


Fig. 7. Semiquantitative score of histological findings, immunoreactivity of staining. The proportion of PCNA-, VEGF-, and PECAM-1-positive cells was scored as 0 (no cells stained positive), 1 (1–10% positive cells), 2 (11–33% positive cells), 3 (34–66% positive cells), or 4 (67–100% positive cells). * $P < 0.05$ one-way ANOVA, Turkey's post-hoc test among groups.

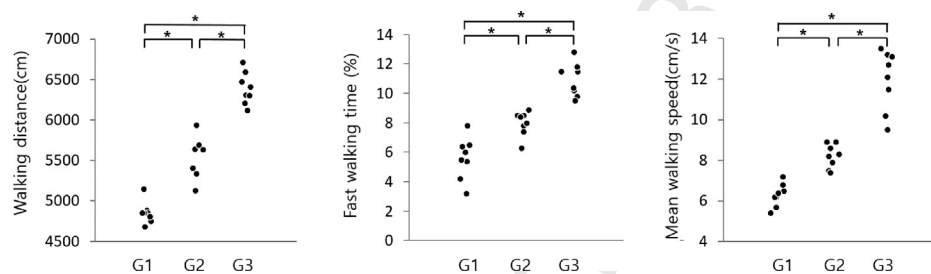


Fig. 8. Motion analysis of rabbits at 4 weeks post-treatment. * $P < 0.05$ one-way ANOVA, Tukey's post-hoc test among groups.

MIC and G1-S groups. The significant differences in gross morphologic changes and tendon tear sizes between MIC-added and Sham MIC-treated groups suggest that MIC-induced VEGF expression improved the regenerative effect of PDRN.

One of the main novel aspects of our approach was the use of musculoskeletal US for US-guided injection. Musculoskeletal US is expected to become a critical interventional tool for regenerative injection therapies because US-guided injections allow stem cells to be selectively administered to the target area [10,34]. Moreover, rather than focusing on the mechanical properties of the regenerated tendon, we conducted motion analysis of the rabbits to evaluate the improvement in functional ability directly [10]. Although motion analysis has not yet been found superior to mechanical testing, which is more frequently used in animal models of rotator cuff tears [21,35], motion analysis is a potentially important tool to assess the therapeutic effect of treatments for FTRCTT based on data from human studies [36].

Chronic RCTTs adversely affect the surgical repair of lesions [37]. Massive FTRCTTs are usually associated with myotendinous retraction, atrophy, and fatty infiltration of muscles, which are poor prognostic factors for surgical outcomes. Therefore, a "chronic" FTRCTT model is needed to accurately assess the clinical utility of PDRN and MIC in humans. For this study, we used a rabbit model of a chronic traumatic RCTT after 6 weeks of trauma. Previous studies of the rabbit supraspinatus muscle have shown fatty degeneration beginning as early as 4 weeks, with a peak at 6 weeks, and slow reversal by 12 weeks [38]. FTRCTT becomes irreparable after approximately 6 weeks because of excessive tendon retraction and muscle atrophy and stiffening [39]. From these previous studies, we selected 6 weeks for establishing chronic injury, although we did not confirm whether typical "chronic" findings were present in tendon injuries [38,40].

There are some limitations of our study. First, we created 5 × 5-mm FTRCTTs just proximal to the insertion site on the left

subscapularis tendon. After each excision was made, each wound was immediately covered with a round silicone tube to induce a chronic rotator cuff tear. Each wound was then closed by using subcutaneous and skin sutures. However, these tears were in the tendon body and not exactly at the insertion site. Second, the FTRCTT model in the present study is a traumatic model, not a spontaneous degenerative model. Third, complete regeneration did not occur. More "complete" rotator cuff healing might have been observed if outcomes were measured at 8 weeks or more, instead of 4 weeks. Fourth, we did not perform a biomechanical test of the regenerative tendon. Fifth, considering that this study was conducted in a relatively short time period, it is necessary to assess the long-term effects of MIC. Sixth, we did not assess the effects of MIC alone on FTRCTT. Finally, additional studies are needed to evaluate the effects of MIC of various frequencies and durations (less than 30 min or more than several hours) for achieving optimal results.

5. Conclusion

In a rabbit model of chronic traumatic FTRCTT, combined therapy of PDRN with MIC was more effective than PDRN alone in terms of gross morphological, histological, and motion analyses. The results of this study regarding the potential of the combination treatment of PDRN and MIC warrant further investigation. To our knowledge, this is the first study to assess the regenerative effects of PDRN and MIC on FTRCTT, and our findings suggest that the physical and biochemical interactions between PDRN and MIC may promote the regeneration of RCTT in a rabbit model.

Funding

This work was supported by a grant from the Research Institute of Medical Science, Catholic University of Daegu (2019).

Disclosure of interest

The authors declare that they have no competing interest.

References

- [1] Yamaguchi K, Ditsios K, Middleton WD, Hildebolt CF, Galatz LM, Teefey SA. The demographic and morphological features of rotator cuff disease. A comparison of asymptomatic and symptomatic shoulders. *J Bone Joint Surg Am* 2006;88:1699-704. <http://dx.doi.org/10.2106/JBJS.E.00835>.
- [2] Castricini R, Longo UG, De Benedetto M, Panfoli N, Pirani P, Zini R, et al. Platelet-rich plasma augmentation for arthroscopic rotator cuff repair: a randomized controlled trial. *Am J Sports Med* 2011;39:258-65. <http://dx.doi.org/10.1177/0363546510390780>.
- [3] Yoon YC, Lee D-H, Lee MY, Yoon S-H. Polydeoxyribonucleotide injection in the treatment of chronic supraspinatus tendinopathy: a case-controlled, retrospective, comparative study with 6-month follow-up. *Arch Phys Med Rehabil* 2017;98:874-80. <http://dx.doi.org/10.1016/j.apmr.2016.10.020>.
- [4] Kim JK, Chung JY. Effectiveness of polydeoxyribonucleotide injection versus normal saline injection for treatment of chronic plantar fasciitis: a prospective randomised clinical trial. *Int Orthop* 2015;39:1329-34. <http://dx.doi.org/10.1007/s00264-015-2772-0>.
- [5] Kwon DR, Park G-Y, Lee SC. Treatment of full-thickness rotator cuff tendon tear using umbilical cord blood-derived mesenchymal stem cells and polydeoxyribonucleotides in a rabbit model. *Stem Cells Int* 2018;2018:7146384. <http://dx.doi.org/10.1155/2018/7146384>.
- [6] Demidova-Rice TN, Durham JT, Herman IM. Wound Healing Angiogenesis: Innovations and Challenges in Acute and Chronic Wound Healing *Adv Wound Care* (New Rochelle) 2012;1:17-22. <http://dx.doi.org/10.1089/wound.2011.0308>.
- [7] Ferroni P, Roselli M, Guadagni F, Martini F, Mariotti S, Marchitelli E, et al. Biological effects of a software-controlled voltage pulse generator (PhyBack PBK-2C) on the release of vascular endothelial growth factor (VEGF). *In Vivo* 2005;19:949-58.
- [8] Sebastian A, Syed F, Perry D, Balamurugan V, Colthurst J, Chaudhry IH, et al. Acceleration of cutaneous healing by electrical stimulation: degenerate electrical waveform down-regulates inflammation, up-regulates angiogenesis and advances remodeling in temporal punch biopsies in a human volunteer study. *Wound Repair Regen* 2011;19:693-708. <http://dx.doi.org/10.1111/j.1524-475X.2011.00736.x>.
- [9] Fu D, Mitra K, Sengupta P, Jarnik M, Lippincott-Schwartz J, Arias IM. Coordinated elevation of mitochondrial oxidative phosphorylation and autophagy help drive hepatocyte polarization. *Proc Natl Acad Sci USA* 2013;110:7288-93. <http://dx.doi.org/10.1073/pnas.1304285110>.
- [10] Park G-Y, Kwon DR, Lee SC. Regeneration of Full-Thickness Rotator Cuff Tendon Tear After Ultrasound-Guided Injection With Umbilical Cord Blood-Derived Mesenchymal Stem Cells in a Rabbit Model. *Stem Cells Transl Med* 2015;4:1344-51. <http://dx.doi.org/10.5966/sctm.2015-0040>.
- [11] Coleman SH, Fealy S, Ehteshami JR, MacGillivray JD, Altchek DW, Warren RF, et al. Chronic rotator cuff injury and repair model in sheep. *J Bone Joint Surg Am* 2003;85-A:2391-402.
- [12] Poltawski L, Johnson M, Watson T. Microcurrent therapy in the management of chronic tennis elbow: pilot studies to optimize parameters. *Physiother Res Int* 2012;17:157-66. <http://dx.doi.org/10.1002/pri.526>.
- [13] Fleischli JG, Laughlin TJ. Electrical stimulation in wound healing. *J Foot Ankle Surg* 1997;36:457-61.
- [14] de Girolamo L, Stanco D, Galliera E, Viganò M, Colombini A, Setti S, et al. Low frequency pulsed electromagnetic field affects proliferation, tissue-specific gene expression, and cytokines release of human tendon cells. *Cell Biochem Biophys* 2013;66:697-708. <http://dx.doi.org/10.1007/s12013-013-9514-y>.
- [15] Vavken P, Arrich F, Schuhfried O, Dorotka R. Effectiveness of pulsed electromagnetic field therapy in the management of osteoarthritis of the knee: a meta-analysis of randomized controlled trials. *J Rehabil Med* 2009;41:406-11. <http://dx.doi.org/10.2340/16501977-0374>.
- [16] Cheng N, Van Hoof H, Bockx E, Hoogmartens MJ, Mulier JC, De Dijkster FJ, et al. The effects of electric currents on ATP generation, protein synthesis, and membrane transport of rat skin. *Clin Orthop Relat Res* 1982;264-72.
- [17] Akai M, Shirasaki Y, Tateishi T. Electrical stimulation on joint contracture: an experiment in rat model with direct current. *Arch Phys Med Rehabil* 1997;78:405-9.
- [18] Lin Y, Nishimura R, Nozaki K, Sasaki N, Kadosawa T, Goto N, et al. Effects of pulsing electromagnetic fields on the ligament healing in rabbits. *J Vet Med Sci* 1992;54:1017-22.
- [19] Nessler JP, Mass DP. Direct-current electrical stimulation of tendon healing in vitro. *Clin Orthop Relat Res* 1987;303-12.
- [20] Dunn SM. Multiple calcium channels in synaptosomes: voltage dependence of 1,4-dihydropyridine binding and effects on function. *Biochemistry* 1988;27:5275-81.
- [21] Byl NN, McKenzie AL, West JM, Whitney JD, Hunt TK, Hopf HW, et al. Pulsed microamperage stimulation: a controlled study of healing of surgically induced wounds in Yucatan pigs. *Phys Ther* 1994;74:201-13 [discussion 213-218].
- [22] Veronesi F, Dallari D, Sabbioni G, Carubbi C, Martini L, Fini M. Polydeoxyribonucleotides (PDRNs) From Skin to Musculoskeletal Tissue Regeneration via Adenosine A2A Receptor Involvement. *J Cell Physiol* 2017;232:2299-307. <http://dx.doi.org/10.1002/jcp.25663>.
- [23] Farmer SE, James M. Contractures in orthopaedic and neurological conditions: a review of causes and treatment. *Disabil Rehabil* 2001;23:549-58.
- [24] Amadori S, Torricelli P, Panzavolta S, Parrilli A, Fini M, Bigi A. Multi-layered scaffolds for osteochondral tissue engineering: in vitro response of co-cultured human mesenchymal stem cells. *Macromol Biosci* 2015;15:1535-45. <http://dx.doi.org/10.1002/mabi.201500165>.
- [25] Squadrito F, Bitto A, Altavilla D, Arcoraci V, De Caridi G, De Feo ME, et al. The effect of PDRN, an adenosine receptor A2A agonist, on the healing of chronic diabetic foot ulcers: results of a clinical trial. *J Clin Endocrinol Metab* 2014;99:E746-53. <http://dx.doi.org/10.1210/jc.2013-3569>.
- [26] Altavilla D, Bitto A, Polito F, Marini H, Minutoli L, Di Stefano V, et al. Polydeoxyribonucleotide (PDRN): a safe approach to induce therapeutic angiogenesis in peripheral artery occlusive disease and in diabetic foot ulcers. *Cardiovasc Hematol Agents Med Chem* 2009;7:313-21.
- [27] Sini P, Denti A, Cattarini G, Daglio M, Tira ME, Balduini C. Effect of polydeoxyribonucleotides on human fibroblasts in primary culture. *Cell Biochem Funct* 1999;17:107-14. [http://dx.doi.org/10.1002/\(SICI\)1099-0844\(199906\)17:2<107::AID-CBF815>3.0.CO;2-#](http://dx.doi.org/10.1002/(SICI)1099-0844(199906)17:2<107::AID-CBF815>3.0.CO;2-#).
- [28] Rathbone MP, Middlemiss PJ, Gysbers JW, DeForge S, Costello P, Del Maestro RF. Purine nucleosides and nucleotides stimulate proliferation of a wide range of cell types. *In Vitro Cell Dev Biol* 1992;28A:529-36.
- [29] Rathbone MP, DeForge S, Deluca B, Gabel B, Laurensen C, Middlemiss P, et al. Purinergic stimulation of cell division and differentiation: mechanisms and pharmacological implications. *Med Hypotheses* 1992;37:213-9.
- [30] Wang DJ, Huang NN, Heppel LA, Extracellular ATP. shows synergistic enhancement of DNA synthesis when combined with agents that are active in wound healing or as neurotransmitters. *Biochem Biophys Res Commun* 1990;166:251-8.
- [31] Chung KI, Kim HK, Kim WS, Bae TH. The effects of polydeoxyribonucleotide on the survival of random pattern skin flaps in rats. *Arch Plast Surg* 2013;40:181-6. <http://dx.doi.org/10.5999/aps.2013.40.3.181>.
- [32] Polito F, Bitto A, Galeano M, Irrera N, Marini H, Calò M, et al. Polydeoxyribonucleotide restores blood flow in an experimental model of ischemic skin flaps. *J Vasc Surg* 2012;55:479-88. <http://dx.doi.org/10.1016/j.jvs.2011.07.083>.
- [33] Chavan AJ, Haley BE, Volkin DB, Marfia KE, Verticelli AM, Bruner MW, et al. Interaction of nucleotides with acidic fibroblast growth factor (FGF-1). *Biochemistry* 1994;33:7193-202.
- [34] Brown MN, Shiple BJ, Scarponi M. Regenerative approaches to tendon and ligament conditions. *Phys Med Rehabil Clin N Am* 2016;27:941-84. <http://dx.doi.org/10.1016/j.pmr.2016.07.003>.
- [35] Pan J, Liu G-M, Ning L-J, Zhang Y, Luo J-C, Huang F-G, et al. Rotator cuff repair using a decellularized tendon slices graft: an in vivo study in a rabbit model. *Knee Surg Sports Traumatol Arthrosc* 2015;23:1524-35. <http://dx.doi.org/10.1007/s00167-014-2923-7>.
- [36] Keener JD, Galatz LM, Stobbs-Cucchi G, Patton R, Yamaguchi K. Rehabilitation following arthroscopic rotator cuff repair: a prospective randomized trial of immobilization compared with early motion. *J Bone Joint Surg Am* 2014;96:11-9. <http://dx.doi.org/10.2106/JBJS.M.00034>.
- [37] Goutallier D, Postel J-M, Gleyze P, Leguilloux P, Van Driessche S. Influence of cuff muscle fatty degeneration on anatomic and functional outcomes after simple suture of full-thickness tears. *J Shoulder Elbow Surg* 2003;12:550-4. <http://dx.doi.org/10.1016/S1058274603002118>.
- [38] Rowshan K, Hadley S, Pham K, Caiozzo V, Lee TQ, Gupta R. Development of fatty atrophy after neurologic and rotator cuff injuries in an animal model of rotator cuff pathology. *J Bone Joint Surg Am* 2010;92:2270-8. <http://dx.doi.org/10.2106/JBJS.I.00812>.
- [39] Derwin KA, Baker AR, Iannotti JP, McCarron JA. Preclinical models for translating regenerative medicine therapies for rotator cuff repair. *Tissue Eng Part B Rev* 2010;16:21-30. <http://dx.doi.org/10.1089/ten.TEB.2009.0209>.
- [40] Quigley RJ, Gupta A, Oh J-H, Chung K-C, McGarry MH, Gupta R, et al. Biomechanical comparison of single-row, double-row, and transosseous-equivalent repair techniques after healing in an animal rotator cuff tear model. *J Orthop Res* 2013;31:1254-60. <http://dx.doi.org/10.1002/jor.22363>.